Structure of Biphenomycin A Derived from Two-Dimensional NMR Spectroscopy and Molecular Modeling

Frank K. Brown,* Judith C. Hempel,† J. Scott Dixon, Salvatore Amato, Luciano Mueller, and Peter W. Jeffs*,‡

Contribution from Smith Kline and French Research Laboratories, P.O. Box 1539, King of Prussia, Pennsylvania 19406-0939. *Received February 1, 1989*

Abstract: The three-dimensional solution structure of the cyclic tripeptide antibiotic biphenomycin has been determined from quantitative nuclear Overhauser effect (NOE) derived distance information employing distance geometry calculations and constrained molecular dynamics energy refinement. The method is shown to be capable of establishing the primary stereochemistry of the chiral centers as 7*R*,8*S*,11*S*,14*S*, the axial chirality of the biphenyl system as *R*, and the conformation of the antibiotic in solution. The strategy employed makes use of NOE-induced strain energy to evaluate model structures after constrained molecular dynamics refinement.

Biphenomycin A (Figure 1), a novel cyclic tripeptide antibiotic,[1] is a member of a new group of antibiotics that shows potent antibacterial activity against gram-positive infections.[2] Studies of the structure of the antibiotic using both chemical and spectroscopic methods led to a structure in which the configuration at the 11-position was defined as *S* (see Figure 1). The assignment of the primary stereochemistry as 7*R*,8*S*,11*S*,14*S* (*RSSS*) was proposed by Kannan and Williams[3] on the basis of interpretation of NMR-derived *J* coupling constants and qualitative nuclear Overhauser effects (NOEs). The presence of a meta-bridged 15-membered ring biphenyl system in the structure of biphenomycin suggests the possibility that the macrocyclic ring may form a conformationally restricted framework that would make the definition of the three-dimensional structure of the antibiotic in solution possible by NMR methods.

In this paper, an analysis is described that makes use of energy-based molecular modeling and precise interproton distances derived from 2D NOE buildup rates to define the stereochemistry and establish the 3D structure of the antibiotic. Structural studies on conformationally restricted cyclic peptides using NMR procedures require NMR methods that are capable of providing accurate interproton distance constraints and computational methods that allow the generation and quantitative comparison of structures based upon the experimental results.[4] The evaluation of structures derived from model building is based upon the ability of energy-minimized structures to simultaneously maintain the experimentally derived constraints.[5] The results reported here suggest that NOE-induced strain energy is a more meaningful basis for evaluation of the structures than the deviations in NOE-derived distances.

Methods

NMR Studies. The NMR experiments were performed on a sample of 4 mg of biphenomycin dissolved in 0.4 mL of DMSO-d_6 and 4% trifluoroacetic acid (TFA). The sample was degassed and sealed in a Wilmad glass tube under argon. The observed chemical shifts and coupling constants are in good agreement with published data[3] with the exception of the two amides at the 9- and 12-positions, which under the different solvent conditions used in our experiments resonate further downfield at 8.78 and 9.14 ppm, respectively. The *J* connectivities were confirmed by COSY experiment and homonuclear mixing experiment[6] using an MLEV-17 mixing interval of 61 ms. *J* couplings were measured in a resolution-enhanced spectrum with a digital resolution of 0.55 Hz.

A series of phase-sensitive NOESY spectra were collected at mixing times of 50, 150, 250, 350, and 500 ms at 26 °C; eight scans were collected in each of the 256 t_1 values; the spectral width was 4545.5 Hz. The NOESY data were processed in the following way: 7-Hz exponential line broadening and 90°-shifted sine-bell apodization were applied in each time domain. The line broadening reduced effects of *J* polarization transfer. Zero-filling was applied in the t_1 domain prior to Fourier transformation resulting in NOESY spectra of 1024 × 1024 points. Volume integrals were calculated over a square of 5 × 5 points centered around manually selected cross peaks.[7] Polynomial base-line correction in both frequency domains of NOESY spectra considerably improved the quality of the volume integral data. The relaxation matrix was calculated from sets of volume integrals by using the formalism described by Olejniczak et al.[8,9] The data collected at a NOE mixing time of 50 ms was used as a reference to compute Γ separately with volume matrices collected at 150, 250, 350, and 500 ms, respectively.

The relaxation matrix elements were converted into interproton distances by assuming that all protons within the macrocyclic ring are affected by the same motional correlation time. The geminal distance of 1.78 Å between protons 15a and 15b was used as an internal distance marker. The relaxation matrix Γ was computed by using the expression

$$\frac{-\ln\{V(\tau_m)\}\{V(\tau_{mref})\} - 1}{\tau_m - \tau_{mref}} = \Gamma$$

where $V(\tau_m)$ is the matrix of the volume intergrals and τ_m and τ_{mref} are the mixing times used in the NOESY experiments. We chose to calculate a truncated time relaxation matrix that includes only protons in the rigid macrocycle. Also excluded were the protons of the N-terminal amino group. This truncation only moderately distorts the computed distances because at the motional correlation time t = 0.8 ns, the magnitude of cross relaxation between protons is still relatively small. Hence, any exclusion of relaxation pathways leads only to moderate distortion of intensities in the truncated system. Further investigation of these effects is still in progress. The resulting upper and lower bounds for interproton distances are given in Table I.

Circular Dichroism Spectra. The UV and CD spectra of biphenomycin in ethanol (c = 0.0926 mg/mL) was obtained on a JASCO-500 instrument. Absorption maxima at λ_{max} 201 nm (ϵ, 47 500) and 262 nm (ϵ, 15 000) in the UV spectrum were accompanied by Cotton effects in the CD spectrum as follows: θ_{210}, 0; θ_{214}, +7500; θ_{220}, 0; θ_{224}, −3800; θ_{229}, 0, θ_{254}, +17 000; $\theta_{282\,infl}$, +1800; θ_{288}, 0; θ_{302}, −5400; θ_{326}, 0.

* To whom correspondence should be addressed.
† Present address: Biosym Technologies, Inc.; 10065 Barnes Canyon Rd., Suite A, San Diego, CA 92121.
‡ Present address: Glaxo, UNC, Venable Hall, Chapel Hill, NC 27514.

(1) (a) Uchida, I.; Ezaki, M.; Shigematsu, N.; Hashimoto, M., *J. Org. Chem.* **1985**, *50*, 1341. (b) Ezaki, M.; Iwami, M.; Yashita, M.; Kohsaka, M.; Aoiki, H.; Imanaka, H. *J. Antibiot.* **1985**, *38*, 1453. (c) Uchida, I.; Shegimatsu, N.; Ezaki, M.; Hashimoto, M. *J. Antibiot.* **1985**, *38*, 1462.
(2) Chang, C. C.; Morton, G. O.; James, J. C.; Siegel, M. M.; Borders, D. B.; Kuck, M. A.; Testa, R. T. Abstracts of Papers, 26th Interscience Conference on Antimicrobial Agents and Chemotherapy, New Orleans, LA, 1986; Abs. No. 920.
(3) Kannan, R.; Williams, D. W. *J. Org. Chem.* **1987**, *52*, 5435.
(4) Fesik, S. W.; Bolis, G.; Sham, H. L.; Olejniczak, E. T. *Biochemistry* **1987**, *26*, 1851.
(5) Clore, G. M.; Gronenborn, A. M. *Protein Eng.* **1987**, *1*, 275.
(6) Bax, A.; Davis, D. G. *J. Magn. Reson.* **1985**, *65*, 355.
(7) FTNMR and DSPACE are available from Hare Research, Inc., Seattle, WA.
(8) The program used was written by one of us (S.A.) and is based upon the same fundamental methods that have been described in ref 9.
(9) (a) Olejniczak, E. T.; Gampe, R. T.; Fesik, S. W. *J. Magn. Reson.* **1986**, *67*, 28. (b) Fesik, S. W.; O'Donnell, T. J.; Gampe, R. T.; Olejniczak, E. T. *J. Am. Chem. Soc.* **1986**, *108*, 3165.

0002-7863/89/1511-7328$01.50/0

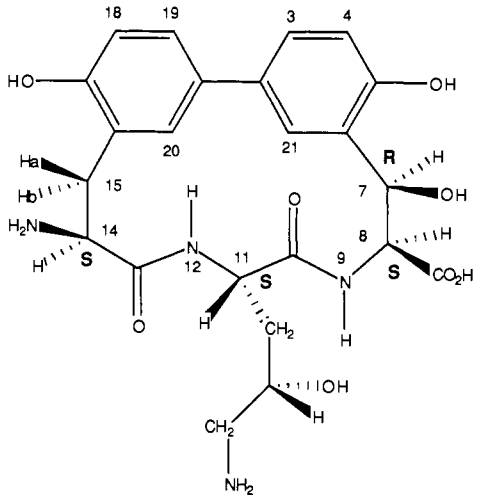

Figure 1. Structure of the cyclic tripeptide antibiotic biphenomycin A. Chiral centers 7*R*,8*S*,11*S*,14*S* are assigned. The numbering convention for the residues of this tripeptide proceeds from the N-terminus (residue 1) to C-terminus (residue 3).

Table I. NOE Distance Constraints for the Macrocyclic Ring of Biphenomycin

proton (template)[a]		bounds, Å	
i	*j*	lower	upper
11 (7)	12 (6)	2.81	2.94
12 (6)	14 (2)	2.33	2.36
12 (6)	15a (3)	2.92	3.73
12 (6)	15b (3)	2.36	2.73
12 (6)	20 (4)	2.90	3.45
9 (12)	21 (16)	2.83	3.15
9 (12)	11 (7)	2.38	2.42
8 (13)	9 (12)	2.76	3.23
20 (4)	21 (16)	2.32	2.36
8 (13)	21 (16)	2.78	3.02
11 (7)	21 (16)	3.46	3.78
15a (3)	20 (4)	2.71	4.14
15b (3)	20 (4)	2.49	2.54
14 (2)	20 (4)	3.09	3.62
7 (14)	8 (13)	2.56	2.62
14 (2)	15a (3)	2.55	2.63
14 (2)	15b (3)	2.48	2.72
9 (12)	12 (6)	3.50	10.00[b]
12 (6)	21 (16)	3.50	10.00
8 (13)	12 (6)	3.50	10.00
9 (12)	20 (4)	3.50	10.00
7 (14)	9 (12)	3.50	10.00
9 (12)	14 (2)	3.50	10.00
7 (14)	21 (16)	3.50	10.00
14 (2)	21 (16)	3.50	10.00
11 (7)	20 (4)	3.50	10.00
8 (13)	20 (4)	3.50	10.00
7 (14)	11 (7)	3.50	10.00
8 (13)	11 (7)	3.50	10.00
14 (2)	11 (7)	3.50	10.00
15a (3)	11 (7)	3.50	10.00
15b (3)	11 (7)	3.50	10.00

[a] Atom numbers are defined in Figure 1 and structural template numbers in Figure 3. [b] Bounds set 3.50–10.00 Å represent an unobserved NOE.

Modeling Studies. The NOE-derived distance data, normal bond angles and bond lengths, planarity restraints for the aromatic rings and peptide bonds, and a single chirality constraint for the C-11*S* center were used as input to the distance geometry program DGEOM[10] to generate 60 conformations of biphenomycin. Coupling constant information was not included in the modeling study. The structures generated include representatives of all eight diastereomers of 11*S*-biphenomycin. Each of these structures was subjected to molecular dynamics refinement using

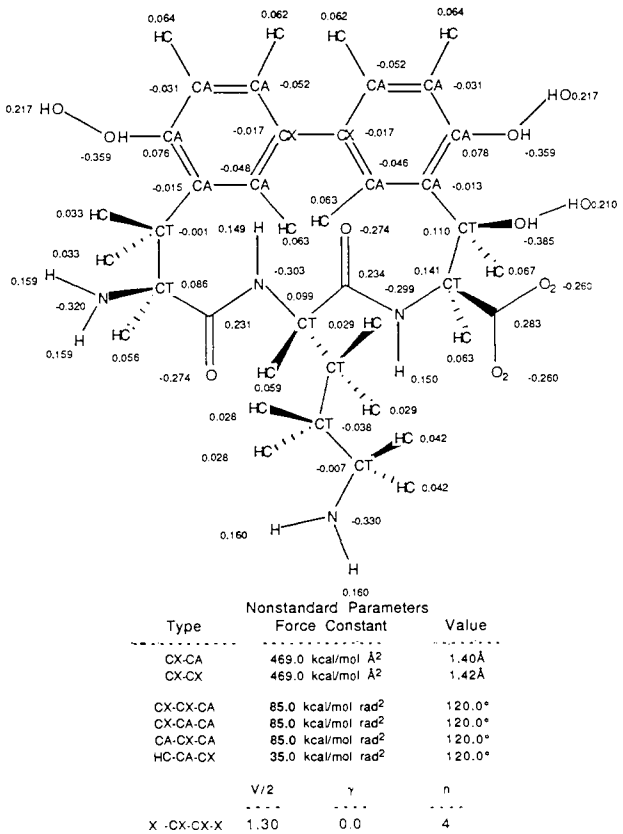

Nonstandard Parameters

Type	Force Constant	Value
CX-CA	469.0 kcal/mol Å^2	1.40Å
CX-CX	469.0 kcal/mol Å^2	1.42Å
CX-CX-CA	85.0 kcal/mol rad^2	120.0°
CX-CA-CA	85.0 kcal/mol rad^2	120.0°
CA-CX-CA	85.0 kcal/mol rad^2	120.0°
HC-CA-CX	35.0 kcal/mol rad^2	120.0°

	V/2	γ	n
X -CX-CX-X	1.30	0.0	4

Figure 2. AMBER 3.0 atom types, charges, and special parameters used in energy minimization and molecular dynamics calculations for biphenomycin A.

the min–md–min strategy described below.

A harmonic constraint (force constant = 100 kcal/(mol Å)) was introduced in AMBER 3.0[11] for interproton distances outside specified bounds. No energy penalty is assessed for interproton distances within bounds. Strain energy introduced by the NOEs was calculated for each structure by using AMBER 3.0 employing charges computed by the method of Gasteiger.[12] The *strain energy* is defined by the difference in energy for the structure refined with NOE constraints (with contributions from the harmonic potential associated with the NOE constraints subtracted out) minus the energy of that structure relaxed, i.e., refined without NOE constraints.

Structures were refined by using a *min–md–min* strategy using AMBER 3.0. Structures were energy minimized, subjected to 5 ps of molecular dynamics at 300 K, and reminimized. This refinement strategy allows localized strain to be redistributed and is referred to as *local refinement*. The use of the min–md–min procedure for searching local conformational space about a distance geometry structure has become a common procedure for the refinement of structures.[4,13] Minimizations (to a root-mean-square gradient of less than 0.01 kcal/mol) and molecular dynamics simulations employed a constant dielectric and no cutoff for nonbond interactions. Charges and force field parameters are given in Figure 2. The torsion angle parameter for the bond connecting the phenyl rings was developed for this study on the basis of three ab initio studies reported for biphenyl.[14-16] The ab initio energy surface defined

(10) Havel, T. F.; Kuntz, I. D.; Crippen, G. M. *Bull. Math. Biol.* **1983**, *45*, 665. The DGEOM program was provided by J. Blaney, Dupont Medical Products Division, Wilmington, DE 19898-0353.

(11) Weiner, S. J.; Kollman, P. A.; Nguyen, E. T.; Case, D. A. *J. Comput. Chem.* **1987**, *7*, 230.

(12) Marsili, M.; Gasteiger, J. *Croat. Chem. Acta* **1980**, *53*, 601. The carboxylate and amine functions were not given formal changes.

(13) The use of MD and distance constraints have been applied to peptides, proteins, and nucleic acids: (a) Clore, G. M., Gronenborn, A. M.; Brunger, A. T.; Karplus, M. J. *J. Mol. Biol.* **1985**, *186*, 435. (b) Kaptein, R.; Zuidreweg, E. R. P.; Scheek, R. M.; Boelens, R.; van Gunsteren, W. F. *J. Mol. Biol.* **1985**, *182*, 197. (c) Nilges, M.; Gronenborn, A. M.; Brunger, A. T.; Clore, G. M. *Protein Eng.* **1988**, *2*, 27. (d) Kessler, H.; Griesinger, C.; Lautz, J.; Muller, A., van Gunsteren, W. F.; Berendsen, H. J. C. *J. Am. Chem. Soc.* **1988**, *110*, 3393. (e) For a general review of conformational searching see: Howard, A. E., Kollman, P. A. *J. Med. Chem.*, **1988**, *31*, 1669.

(14) McKenney, J. D.; Gottschalsk, K. E., Petersen, L. THEOCHEM **1986**, *13*, 445.

(15) Bredas, J. L.; Strret, G. B.; Themans, B.; Andre, J. M. *J. Chem. Phys.* **1985**, *83*, 1323.

Table II. NOE-Induced Strain Energy (kcal/mol) and Percent NOE Deviation as a Function of NOE Force Constant (kcal/(mol Å))

chirality	strain energy[a]			dev in NOE,[b] %		
7,8,11,14	100	50	10	100	50	10
RSSS	4.3	4.5	2.2	0.08	0.12	0.29
SSSS	13.1	12.4	5.2	0.05	0.10	0.29
RSSR	18.0	13.1	7.6	0.08	0.21	0.40

[a] For the low-energy conformers defined in Table IV. [b] The maximum deviation defined by an NOE outside distance bounds relative to the range of that NOE.

Table III. NOE-Induced Strain Energy[a] (kcal/mol) and Biphenyl Ring Twist as a Function of the Biphenyl Torsional Parameter (X-CX-CX-X)

chirality	parameter no. 1[b]		parameter no. 2[c]	
7,8,11,14	strain energy	twist	strain energy	twist
RSSS	4.3	−43.0	2.8	−37.0
SSSS	13.1	40.0	13.6	33.6
RSSR	18.0	42.8	17.3	36.7

[a] For the lowest energy conformer defined in Table IV. [b] For parameter no. 1 ($V/2$ = 1.30, γ = 0.0, n = 4) the relative energies for the biphenyl twist at 0°, 45°, and 90° are 3.9, 0.0, and 2.0 kcal/mol, respectively. This mimics the potential energy surface given in ref 14. This parameter was used to calculate strain energies in Table IV. [c] For parameter no. 2 ($V/2$ = 1.75, γ = 0.0, n = −4; $V/2$ = 2.80, g = 180.0, n = 2) the relative energies for the biphenyl twist at 0°, 45°, and 90° are 1.2, 0.0, and 4.5 kcal/mol. This mimics the potential energy surface given in ref 16.

by McKenney et al.[14] was used to define the torsion parameter given in Figure 2. This energy surface defines the dihedral angle for the low-energy structure of the molecule to be closest to that observed in the gas phase (approximately 42°).[17]

Strain energy was also calculated for each member of this set of 60 structures by reintroducing NOE constraints into the structures after they had been refined without constraints. The force constant on the NOE constraints was increased linearly from 0 to 100 kcal/(mol Å) over a 5-ps molecular dynamics simulation, followed by minimization with the force constant at 100 kcal/(mol Å). This *slow-growth technique* was also used to assess structural implications of a smaller and more qualitative NMR data set previously reported[3] for this molecule by Kannen and Williams.

In addition, 10 structures of biphenomycin consistent with the NOE constraints given in Table I were obtained by using the DSPACE distance geometry program.[7] In a study of this type it is always a concern whether an adequate sampling of structures has been made. In this particular study the validation of the findings using different local refinement strategies and two different distance geometry programs (DSPACE and DGEOM) provides confidence that the best structure has been found (vide infra).

To determine the effect of the magnitude of the force constant imposed for NOE constraints in the calculation of strain energy, values of 50 and 10 kcal/(mol Å) were also used in a min-md-min refinement procedure of the lowest energy 7*R*,8*S*,11*S*,14*S* (*RSSS*), 7*S*,8*S*,11*S*,14*S* (*SSSS*), and 7*R*,8*R*,11*S*,14*R* (*RSSR*) conformers identified in this study. A force constant of 50 kcal/(mol Å) still distinguishes these isomers, but with somewhat larger NOE violations than are allowed by a force constant of 100 kcal/(mol Å) (Table II). At 10 kcal/(mol Å) the difference in the strain energy is small, and the violations of the NOE distances are large. Thus, a force constant of 50 kcal/(mol Å) could have been used in the strain energy evaluation procedure, but a force constant of 10 kcal/(mol Å) on the NOE constraints could not.

The effect of the torsional parameter developed for the biphenyl rotation on the calculated strain energies was examined by using a min-md-min procedure for the lowest energy *RSSS*, *SSSS*, and *RSSR* conformers identified in this study with and without NOE constraints, employing an alternate torsional parameter developed by using the ab initio potential energy surface reported by Almlof.[16] The strain energies calculated are relatively insensitive to this parameter choice (Table III). The dihedral angles of the biphenyl unit obtained after minimization differ by 10° or more for the torsional parameters developed by using the McKenney et al.[14] and Almlof[16] potential energy surfaces but lie within the allowed torsion angle range as defined by the NOE data. Therefore, in this study, the interpretation of the results is insensitive to the choice of parameter for the biphenyl torsion.

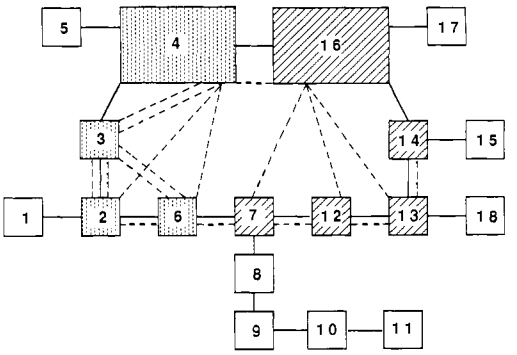

Figure 3. NOE data set. Blocks represent structural templates (sets of atoms whose internal geometry is independent of molecular conformation). Solid lines represent the rotatable bonds of the molecule. Dotted lines represent NOEs (Table I). The identity of each structural template is apparent from a comparison of Figures 1 and 3. Peptide linkages are assigned as a single structural template since the peptide linkages do not interconvert between cis and trans geometries. The peptide bonds of biphenomycin A are trans. Conformational domains defined[20] by the NOEs are distinguished by shaded blocks.

The energy calculations in this study do not include solvent. Although the effect of solvent on total energy of a molecule in solution is difficult to determine, it is possible to estimate differences in interaction energy of various structures by calculating their solvent-accessible surface.[18] When this calculation was performed (supplementary material (see the paragraph at the end of the paper)), the exposed hydrophobic and hydrophilic surface for each diastereomer was found to be very similar. Thus, the interaction energy of these isomers with solvent should also be very similar and energy calculations in the gas phase should provide a reliable representation of the *relative energies* of the structures in solution.

Results and Discussion

NMR Spectroscopy. The proton chemical shift assignments of biphenomycin were readily confirmed by DQ-COSY and homonuclear mixing experiments and were in good agreement with previous results.[3] The NOESY spectra were collected at five different mixing times to allow the use of buildup rates from the NOE intensities to calculate accurate interproton distances through the use of a multispin relaxation matrix program.[8,9] The results of the distance calculation are restricted to the protons on the macrocyclic ring, which is relatively rigid and is assumed to have a single correlation time to describe the motional behavior of the attached protons. The distance bounds were determined from a calculation based upon the use of the intensities from the NOE cross relaxation between the methylene protons at H-15a and H-15b using 1.78 Å as the internuclear distance for internal calibration.

A qualitative picture of how the NOE-derived distance information is distributed within the biphenomycin structure is shown graphically in Figure 3. Structural templates portrayed in this diagram represent sets of atoms contained within structural units whose internal conformation is invariant. The solid lines linking the structural templates in Figure 3 represent rotatable bonds. The NOEs are concentrated in two distinct domains[19,20] localized in the N-terminus (residue 1) and the C-terminus (residue 3) residues. The distance data (Table I) that is portrayed in Figure 3 was used to generate preliminary models of biphenomycin using the DSPACE and DGEOM distance geometry algorithms. Structures obtained were subjected to refinement and analysis as described in the strategies that follow.

Distance Geometry. Molecular Dynamics. Strain Energy. Models of the eight possible diastereomers of 11*S*-biphenomycin were generated in a set of 60 structures produced with DGEOM. After min-md-min refinement with NOE-imposed distance

(16) Almlof, J. *Chem. Phys.* **1974**, *6*, 135.
(17) Bastiansen, O. *Acta Chem. Scand.* **1949**, *3*, 408.
(18) Connelly, M. L. *Science* **1983**, *221*, 709.
(19) Hempel, J. C. *J. Am. Chem. Soc.* **1989**, *111*, 491.
(20) Hempel, J. C.; Brown, F. K. *J. Am. Chem. Soc.*, preceding article in this issue.

Table IV. NOE-Induced Strain Energy (kcal/mol) for the Lowest Energy Conformer by Stereoisomer

chirality		total energy[a]		strain energy	
7,8,11,14	N^b	constrained	unconstrained	local refinement[c]	slow growth[d]
RSSS	5	−20.2	−24.5	4.3	4.6
SSSS	2	−10.8	−23.9	13.1	12.0
RSSR	12	−6.9	−24.9	18.0	17.6
RRSS	10	−4.1	−23.6	19.5	19.4
SRSS	2	−6.5	−20.6	14.1	14.0
RRSR	8	8.9	−24.4	33.3	33.2
SRSR	2	−3.8	−20.5	16.7	34.3[e]
SSSR	19	−5.7	−23.8	18.1	18.5

[a] The *constrained* energy tabulated is for the lowest energy conformer for each stereoisomer after min–md–min with distance constraints. The *unconstrained* is the energy of that conformer after min–md–min without distance constraints. [b] The number of DGEOM structures generated in this study for each stereochemistry. [c] Constrained total energy − unconstrained total energy. [d] Total energy after slow growth − unconstrained energy. [e] The conformer is trapped in a high-energy local minimum during the molecular dynamics cycle of the slow growth procedure.

constraints, the lowest energy structures for the *RSSS*, *SSSS*, and *RSSR* diastereomers showed *no significant deviations* in internuclear H–H distances from the NOE-derived distances (Table II). *Thus, these models are indistinguishable on the basis of the criterion of NOE distance violation.* To differentiate the structures, we explored whether the strain energy introduced by the NOE-derived distance constraints would permit a clear decision to be made in favor of one model.

The strain energy calculated for the *lowest energy* conformer of each of the eight diastereomers of 11*S*-biphenomycin is reported in Table IV. The strain energy values calculated by removing the NOE constraints and allowing the structures to relax during the min–md–min procedures agree within 1–2 kcal/mol with the values obtained by slowly increasing the force constant on the NOE constraints in the fully minimized structure. The only exception to this observation is for the *SRSR* structure, where the side chain of residue 2 is trapped inside the ring portion of the biphenomycin molecule during the molecular dynamics cycle of the refinement procedure. The strain energy introduced by the NOE constraints is lowest for the *RSSS* isomer, at 4.3 kcal/mol. Next is the *SSSS* isomer with a strain energy of 13.1 kcal/mol. Thus, a consideration of strain energy reveals a clear preference for 7*R*,8*S*,11*S*,14*S*-biphenomycin as the structure of the antibiotic. The results of the strain energy calculations for the full set of 60 DGEOM structures are included in the supplementary material.

The strain energy calculated for the model structures occurs as a consequence of NOE-derived distances that cannot be satisfied when the model is relaxed. An analysis of the strain energy for the lowest energy conformer identified for each diastereomer is given in Table V. The energy of the structure after local refinement with distance constraints is factored by residue into bond, angle, dihedral, and nonbond components. In the *RSSS* structure (the least strained of the models summarized in Table III) interproton distances between protons 12-15b (linking structural templates 6 and 3 in Figure 3) and 12-20 (linking structural templates 6 and 4) prefer to be slightly shorter when relaxed than is "permitted" by the NOE data. This results in the strain energy for this structure being localized in residue one. NOE induced strain in the *SSSS* conformer is concentrated in residue three. The strain energy is localized in residue three because the *SSSS* and *RSSS* diastereomers differ only in chirality at C-7, the β carbon of residue 3. The *SRSR* and *RSSS* diastereomers differ at C-7, C-8, and C-14, and the strain introduced by the NOE constraints for the SRSR conformer extends throughout the macrocyclic ring. This analysis emphasizes that the NOEs that define stereochemistry for this molecule are interrelated at a residue level. The NOE-induced strain is distributed within structural domains defined[19,20] by NOEs clustered in residue 1

Table V. NOE-Induced Strain Energy (kcal/mol) by Residue for the Lowest Energy Conformer by Stereoisomer

centers	bond energy				angle energy				dihedral energy				VDW energy				electrostatic energy				total strain
7,8,11,14	res 1[b]	res 2	res 3	total	res 1	res 2	res 3	total	res 1	res 2	res 3	total	res 1	res 2	res 3	total	res 1	res 2	res 3	total	energy[a]
RSSS	0.08	0.01	0.00	0.09	1.62	0.20	0.26	2.08	0.36	0.20	0.62	1.18	0.42	−0.06	−0.32	0.04	0.21	0.60	−0.07	0.74	4.3
SSSS	0.32	0.06	0.14	0.52	1.38	0.44	2.73	4.55	0.58	0.82	1.83	3.23	0.87	0.02	0.54	1.43	0.27	0.81	3.53	4.61	13.1
RSSR	0.23	1.36	0.16	1.75	2.20	3.72	0.98	6.90	1.48	0.34	0.36	2.18	1.24	1.19	0.25	2.68	−0.42	4.49	0.56	4.63	18.0
RRSS	0.24	0.02	1.59	1.85	2.06	0.22	4.92	7.20	0.87	0.94	1.04	2.85	0.43	0.27	4.64	5.34	−2.03	0.59	4.97	3.53	19.8
SRSS	0.13	0.08	1.59	1.80	1.56	1.59	4.24	7.39	0.12	−0.08	−1.38	−1.34	0.05	1.62	2.77	4.44	−0.95	1.09	2.83	2.97	14.1
RRSR	0.36	1.29	1.52	3.17	2.42	5.18	8.24	15.84	0.49	0.50	−0.53	0.46	2.87	1.67	4.10	8.64	0.53	2.42	7.68	10.63	33.3
SRSR	0.82	0.18	−0.01	0.99	5.53	2.43	0.17	8.13	3.89	2.02	2.23	8.14	−0.36	−0.90	−0.92	−2.18	−0.79	0.62	−0.81	−0.98	16.7
SSSR	0.28	0.89	0.11	1.28	1.88	1.98	2.87	6.73	0.12	−0.23	2.47	2.36	2.17	1.22	−0.38	3.01	−1.23	2.65	3.01	4.43	18.1

[a] The components shown do not sum to the total strain energy since strain energy resulting from interactions between residues is not tabulated. [b] Residue 1 = residue at N-terminus, residue 2 = central residue, residue 3 = residue at C-terminus.

Table VI. Comparison of Dihedral Angles Predicted from J Coupling Constants and Torsion Angles Measured for the Lowest Energy Conformer by Stereoisomer

coupling const	calc ϕ,[a] deg	*RSSS*	*SSSS*	*RSSR*	*RRSS*	*SRSS*	*RRSR*	*SRSR*	*SSSR*
$J_{7,8}$ = 0.0	±90	−79.7	−105.0	−71.6	47.1	66.6	40.7	84.0	−106.9
$J_{8,9}$ = 10.0	±163	175.1	164.2	−172.4	104.8	−74.9	77.5	195.8	184.9
$J_{11,12}$ = 9.6	±159	−151.3	−167.3	−21.7	184.4	−137.8	76.3	142.5	−75.0
$J_{14,15a}$ = 3.0	±62	63.5	60.7	−63.9	−68.9	64.5	−102.9	−101.7	60.4
	±109								
$J_{14,15b}$ = 6.5	±37	−54.6	−57.6	52.2	50.5	52.8	141.2	142.7	−57.8
	±130								

[a] Calculated from the equations proposed by: Bystrov, V. F. In *Nuclear Magnetic Resonance Spectroscopy*; Emsley, J. M., Feeney, J., Sutcliffe, L. H., Eds.; Pergamon Press: Elmsford, NY, 1976; Vol. 10, p 41. The values reported are consistant with those reported by Kannan and Williams.[3]

and residue 3 as illustrated in Figure 3 and discussed in greater detail in a companion paper.[20]

Distance Geometry. Molecular Dynamics. Iterative Refinement. An additional 10 structures of 11*S*-biphenomycin were generated from the NOE-derived distance bounds by using the distance geometry program DSPACE rather than DGEOM. These structures were subjected to gradient refinement followed by molecular dynamics in an iterative fashion until a local minimum was reached. Each of the residues in the resulting structures that showed NOE distance violations was subjected to randomization within a sphere of 2.5 Å followed by error refinement. (These algorithms are integral to the DSPACE program.) The study generated the *RSSS* isomer as the structure containing the minimum number of violations and lowest error function identified by the procedure. The structure obtained was indistinguishable after AMBER 3.0 min–md–min refinement from the structure defined by the more comprehensive study outlined above. Without further examples, it is not clear whether this approach can be used with the same level of confidence as the more systematic and rigorous procedure described in the previous section.

J Coupling and Circular Dichroism Spectra of Biphenomycin. A comparison of torsion angle values derived from the observed coupling constants and the value of the corresponding torsion angles for the low-energy conformers of all eight diastereomers of 11*S*-biphenomycin reveals that the *RSSS*, *SRSR*, and *SSSS* stereoisomers are consistent with the predictions made from the coupling constants (see Table VI). This observation supports the assignment of *RSSS* stereochemistry for this molecule (vide supra).

It is apparent from an examination of the computer-generated three-dimensional models for the eight isomers of biphenomycin identified in Table IV not only that the aromatic rings of the biphenyl chromophore are twisted relative to one another (by 35–47°) but that the *R* and *S* axial chirality of twist are represented in this series. Interestingly, the axial chirality of the biphenyl rings for the *RSSS* model is *R* while that for the *SSSS* isomer model (the model next highest in strain energy) is *S*. One might ask therefore whether the circular dichroism spectrum of the antibiotic can be interpreted to establish the chirality of the biphenyl chromophore twist in solution.

The circular dichroism spectrum of the antibiotic exhibits positive and negative Cotton effects at 282 and 302 nm, respectively, associated with the aromatic chromophore. However, the intensities of these features are weak and unbalanced due presumably to conjugation between the aromatic rings. Application of the exciton chirality method[21] to determine the absolute twist for the biphenyl rings of biphenomycin is therefore precluded. Conjugation is consistent with a biphenyl ring twist of 35–47°.[14-16]

Conclusion

Two strategies using quantitative NOE-derived distance information and distance geometry to build model structures, followed by energy minimization and molecular dynamics to refine these structures, demonstrate a clear preference for *RSSS* stereochemistry for biphenomycin A and define the solution conformation of the molecule depicted in Figure 4. As is implied

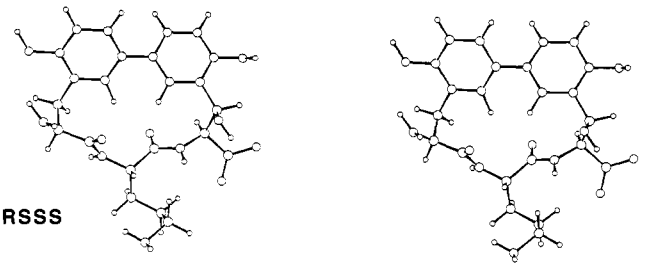

Figure 4. Biphenomycin A solution conformation model. This conformation and stereochemistry (7*R*,8*S*,11*S*,14*S*) was determined to be the best fit to the NOE data presented in Table I. Coordinates are included as supplementary material. A consideration of the NOE data as presented in Figure 3 reveals that the conformation of the side chain of residue 2 is not defined by the data. The side-chain conformation illustrated in this model is therefore simply one of a range of low-energy conformations available to the side chain in solution.

by the representation of the NOE data presented in Figure 3, the conformation presented for the side chain of residue 2 in the solution conformation model is not defined by experiment and is simply one of many accessible low-energy conformers. The NMR studies of this molecule indicate that biphenomycin A is characterized by a single conformation of the macrocyclic ring. The mobility expected for the hydroxyornithine side chain (residue 2) is also clearly indicated by decreased NOE intensity of the geminal hydrogens in the side chain relative to the ring methylene pair at position 15.

Our attempts to define the stereochemistry of the antibiotic using the J coupling coefficients and a smaller and less quantitative set of NOEs previously reported by Kannan and Williams[3] did not lead to a unique solution. Despite having substituted quantitative distance data for the qualitative information in the smaller data set, the systematic "slow-growth" energy-based modeling method *cannot distinguish* biphenomycin structures differing in configuration at the 14-position. This finding is supported by an analysis of the distribution of the Kannan and Williams data across the structural templates of the molecule that establishes that there is not enough information in this data set to unambiguously define the chirality at position 14. This analysis is discussed in greater detail in a companion paper.[20] Furthermore, it is likely that the increased distance bounds implicit in the qualitative NOEs used by Kannan and Williams may have yielded other structures that are in agreement with their data. Although these authors proposed the 7*R*,8*S*,11*S*,14*S* primary stereochemistry from their NOE and J coupling data and interactive modeling, without the benefit of accurate distance information or energy considerations, their results indicate only that a structure consistent with the data was found. Such a finding becomes significant only when other possible structures are systematically excluded.

A search of the conformation space defined by the NMR data for a molecule the size of biphenomycin almost certainly requires computation-based search procedures to deal with the large number of structures to be considered. Two computational modeling strategies were used in this study. Both converged to the same assignment of stereochemistry and macrocyclic ring conformation for the antibiotic. In the more systematic of the two studies, initial structures derived from distance geometry were subjected to constrained energy minimization by using molecular

(21) Harada, N., Nakanishi, K. *Circular Dichroic Spectroscopy—Exiton Coupling in Organic Stereochemistry*; University Science Books: Mill Valley, CA, 1983.

dynamics. An analysis of the resulting structures has been developed employing a detailed evaluation of the strain energy that is imposed by the NOE derived distance constraints.

This NOE-induced strain energy analysis is shown to be more useful in discriminating structural models developed for biphenomycin than analyses that use deviations from NOE distance bounds or torsion angles derived from J coupling as the criteria. *We conclude that the most effective criterion for the evaluation of model structures is not how closely a relaxed structure matches the distance data, but rather how much strain is induced when the structure does fit the NOE data.*

Acknowledgment. We thank Dr. Mine, Fujisawa Pharmaceutical Co., Ltd., for a sample of biphenomycin A. We are indebted to Dr. D. Hare (Hare Research Inc.) for his distance geometry program, DSPACE, and to Drs. G. M. Crippen and J. Blaney for providing modified versions of the distance geometry program.

Registry No. Biphenomycin A, 100296-21-7.

Supplementary Material Available: Total energies for the 60 structures from the DGEOM study when relaxed and when constrained (both from the local refinement and slow growth procedures using the data in Table I and from slow growth with the subset of Table I corresponding to the Kannan and Williams[3] data set), the solvent-accessible surfaces of the low-energy structures given in Table IV, and the coordinates for the *RSSS* solution conformation model (6 pages). Ordering information is given on any current masthead page.

Theoretical Studies of High-, Intermediate-, and Low-Spin Model Heme Complexes

Frank U. Axe, Charles Flowers, Gilda H. Loew,* and Ahmad Waleh*

Contribution from The Molecular Theory Laboratory, The Rockefeller University, 701 Welch Road, Suite 213, Palo Alto, California 94304. *Received February 25, 1988*

Abstract: We report here the systematic application of a semiempirical INDO/S-RHF (restricted Hartree-Fock) open-shell procedure to calculate the relative energies, electron and spin distributions, and Mössbauer quadrupole splittings for the low-lying spin states of a series of eighteen high- ($S = {}^5/_2$), intermediate- ($S = {}^3/_2$), and low-spin ($S = {}^1/_2$) ferric heme complexes for which crystal geometries are known and the ground spin states can be inferred from the observed electromagnetic properties. In general, the predicted ground spin state and the calculated energies of the other spin states relative to it are quantitatively consistent with the observed effective magnetic moments, ESR spectra, and the Mössbauer quadrupole splitting spectra for the compounds studied. For all the high-spin compounds studied, the doublet states are predicted to be thermally inaccessible, being 14-35 kcal/mol higher in energy than the sextet state. The calculated energy separation between the quartet and sextet states are significantly high in the five-coordinated compounds (~11 kcal/mol) and decreases to less than 5 kcal/mol in the six-coordinated compounds. For diaquo and diethanol ferric heme complexes, we calculate near-degenerate $S = {}^3/_2$ and $S = {}^5/_2$ states. The intermediate-spin compounds exhibit a quartet ground state, consistent with experimental observations, with an energy separation of 2-7 kcal/mol from the sextet and about 20 kcal/mol from the doublet states. The calculated results for the low-spin complexes all exhibit rather pure $S = {}^1/_2$ ground states. Only for complexes exhibiting different crystal geometries for the same axial ligands are the sextet and quartet states close enough in energy to the doublet state that interaction with these spin states of higher multiplicity may be significant. The results obtained for all complexes studied allow insights into the effect of geometry and axial ligand(s) on the relative energies and observable properties of various spin states of ferric heme complexes.

The presence of low-lying states of different multiplicities is a characteristic feature of heme active sites, as evidenced by their observed electromagnetic properties and by changes in spin states that occur during their biological function.[1-5] Studies of model heme complexes have revealed that the relative ordering of the manifold of low-lying spin states depends greatly upon the axial ligand(s) and the geometry of the complex.[6-9] A parallel dependence is also observed in intact heme proteins.[5] Therefore, theoretical identification and characterization of such spin states are very important in understanding the origin of electromagnetic properties and spectra of the heme proteins and the influence of chromophore geometry and axial ligands on their biological functions. Spin-state changes frequently occur during the biological function of heme proteins, accompanied by geometry changes or changes in axial ligands of the heme unit. Thus, it is important to establish a 1:1 correspondence between geometry, nature of axial ligand, and spin-state manifold that would allow spin to be deduced from geometry and vice versa.

We have, in the past, successfully applied[10] a semiempirical INDO/S method[11,12] to characterize the ground and excited states of various closed-shell model heme complexes. Now, by employing a restructed Hartree-Fock (RHF) and a generalized CI formalism,[13-15] the application of the INDO/S method can be ex-

* Authors to whom correspondence should be addressed.

(1) (a) Poulos, T. L. *Adv. Inorg. Biochem.* **1988**, *7*, 1-36. (b) Poulos, T. L.; Finzel, B. C. In *Peptide and Protein Reviews*; Hearn, M. T. W., Ed.; Marcel Dekker: New York, 1984; Vol. 4, p 115.
(2) Dunford, H. B.; Stillman, J. S. *Coord. Chem. Rev.* **1976**, *19*, 187.
(3) Schonbaum, G. R.; Chance, B. In *The Enzymes*, 3rd ed.; Boyer, P. D., Ed.; Academic Press: New York, 1976; pp 295-332.
(4) Hewson, W. D.; Hager, L. P. In *The Porphyrins*; Dolphin, D., Ed.; Academic Press: New York, 1979; Vol. 7, pp 295-332.
(5) Dawson, J. H.; Eble, K. S. *Advanced Inorg. Bioinorg. Mech.* **1986**, *4*, 1.
(6) Scheidt, W. R.; Reed, C. A. *Chem. Rev.* **1981**, *81*, 543.
(7) Williams, R. J. P. *Fed. Proc., Fed. Am. Soc. Exp. Biol.* **1961**, *20*, 5.
(8) Hoard, J. L.; Hamor, M. J.; Hamor, T. A.; Caughey, W. S. *J. Am. Chem. Soc.* **1965**, 2312.
(9) Hoard, J. L. *Science* **1971**, *174*, 1295.
(10) Loew, G. H. In *Iron Porphyrins, Part I*; Lever, A. B. P., Gray, H. B., Eds.; Addison-Wesley: Reading, MA, 1983; pp 1-87.
(11) Ridley, J.; Zerner, M. *Theor. Chim. Acta* **1973**, *32*, 111. Ridley, J. E.; Zerner, M. C. *Theor. Chim. Acta* **1976**, *42*, 223. Bacon, A. D.; Zerner, M. C. *Theor. Chim. Acta* **1979**, *53*, 21.
(12) Zerner, M. C.; Loew, G. H.; Kirchner, R. F.; Muller-Westerhoff, U. T. *J. Am. Chem. Soc.* **1980**, *102*, 589.
(13) Edwards, W. D.; Zerner, M. C. *Theor. Chim. Acta* **1987**, *72*, 347.

0002-7863/89/1511-7333$01.50/0